The analysis of the data obtained at helium temperatures is considerably simplified by the assumption of strong statistical degeneracy. An expression for the electron concentration is obtained as follows. For a spherically symmetrical conduction band the electron concentration is given by

$$n = k_F^3/3\pi^2 \quad , \tag{1}$$

where k_F is the electron wave vector at the Fermi surface.

The $E(\vec{k})$ relationship for the conduction band from $\vec{k}\cdot\vec{p}$ theory for the case of kP_K and E_g very much less than the spin-orbit splitting energy is[4]

$$E(k) = \frac{\hbar^2 k^2}{2m_0} + \frac{E_g + (E_g^2 + \frac{8}{3}k^2P_K^2)^{1/2}}{2} \quad , \tag{2}$$

where P_K is the Kane matrix element, and the energies are measured from the valence-band edge. The first term is negligible for the narrow-gap alloys. By replacing $E(k)$ and k by their values at the Fermi level, E_F and k_F, and rearranging, we obtain (for $E_F > E_g$)

$$k_F^2 = \frac{3}{2P_K^2} E_F(E_F - E_g) \ . \tag{3}$$

Combining Eqs. (1) and (3) yields

$$n^{2/3} = \left(\frac{1}{3\pi^2}\right)^{2/3} \frac{3}{2P_K^2} E_F(E_F - E_g) \ . \tag{4}$$

On substituting $E_g = E_0 + \alpha P$ this becomes

$$n^{2/3} = \left(\frac{1}{3\pi^2}\right)^{2/3} \frac{3}{2P_K^2} E_F(E_F - E_0 - \alpha P) \ . \tag{5}$$

The expression is valid in both the normal- and inverted-band-structure regions, provided that the correct sign is used for E_0 (E_0 is negative for the inverted band structure).

The electron concentrations obtained experimentally at 4.2 °K for the three samples are shown in Fig. 8, plotted as $n^{2/3}$ vs P. A straight line is obtained in each case, indicating that the position of the Fermi energy relative to the valence-band edge is independent of pressure. The slope of the line yields $\alpha E_F/P_K^2$. E_F is found by taking $\alpha = 7\times10^{-3}$ eV/kbar (the value obtained at 77 °K) and $P_K = 8.4\times10^{-8}$ eV cm.[5] E_0 is then obtained from E_F and the intercept on the pressure axis. The values of E_F and E_0 found in this way are given in Table II. The small difference in E_0 for samples 7B1 and 7B, which were taken from the same slice of the parent crystal, could be due to an undetected difference in alloy composition. The required difference in x is 0.004, which is within the experimental error of the microprobe analysis. Values for E_0 calculated for the measured values of x from empirical expressions[8,30] for $E_g(x,T)$ are also listed in Table II. Those obtained from the expression given by Wiley and Dexter,[8] which assumes a linear dependence of energy gap on both composition and temperature, agree well with the experimental values.

DISCUSSION

According to the $\vec{k}\cdot\vec{p}$ analysis, at 4.2 °K the position of the Fermi level, with respect to the valence band, is independent of pressure in all three samples. It is situated more than 9 meV (or $25kT$) above the conduction-band edge at zero pressure. This must be reconciled with hole concentrations greater than 10^{17} cm^{-3} which are measured in samples 7B1 and 8B at 4.2 °K. The high values for the np product cannot be due to an overlap of the conduction and valence bands, since the high hole density is not observed in sample 7B.

A possible model to account for the observed behavior is shown in Fig. 11. The energy-band structure near the zone center is shown as a function of pressure for an alloy which is semimetallic at zero pressure. We show an acceptor level situated above the heavy-mass valence-band edge, whose energy with respect to the valence-band edge does not change with pressure. Thus, below the pressure P_c the acceptor states lie within the conduction band. Evidence for discrete impurity states lying within a band of states has been obtained in other materials. In CdTe the

TABLE II. Values at 4.2 and 77 °K for the energy gap at zero pressure and the Fermi energy.

Sample	T (°K)	x	E_F (meV)	E_0 (meV)	E_0 calculated (meV) (Ref. 8)	(Ref. 30)
7B	4.2	0.149 ± 0.005	9	−16	−14 ± 9	−45 ± 9
7B1	4.2	0.149 ± 0.005	16	−10	−14 ± 9	−45 ± 9
8B	4.2	0.138 ± 0.005	20	−33	−35 ± 9	−63 ± 9
7B	77	0.149 ± 0.005	23[a]	−8.0	+11.6	−15
			31[b]	+2.0	+11.6	−15

[a]Calculated assuming a hole mass $m_h^* = 0.3$

[b]Hole mass $m_h^* = 0.7$.

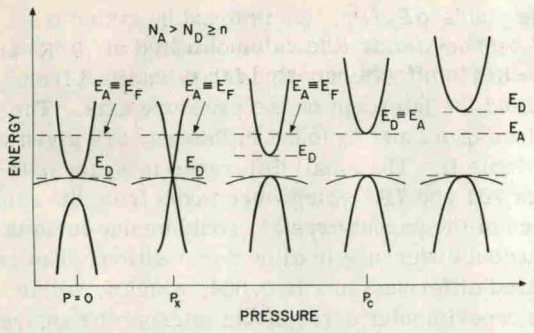

FIG. 11. Schematic of the band structure of $Hg_{1-x}Cd_xTe$ at the zone center as a function of pressure. N_A and N_D are the densities of acceptors and donors, respectively. The electron density n is $\int_{E_c}^{E_f} g(E)dE$, where $g(E)$ is the density of states in the conduction band and E_c the energy at the band edge.

donor states associated with Ga, In, Cl, and Br are believed to lie above the Γ_6 minimum[31] and in $GaAs_{1-x}P_x$:N a resonant state of the N isoelectric trap has been shown to exist above the conduction-band minimum for $x = 0.19$ and 0.21.[32]

To explain the results for sample 7B, we assume that this sample is compensated with a donor density which is greater than the number of conduction-band states below the acceptor level (but less than the density of acceptor states). The donor level is at the bottom of the conduction band. In this situation the Fermi energy is pinned at the acceptor level. With applied pressure the electron concentration falls as the number of states below E_A decreases and becomes zero at a pressure P_c, where E_g is equal to E_A. The value for E_A from Table II is 9 meV.

We suggest that in samples 7B1 and 8B the acceptor density is high enough to form a band of states in which "metallic" impurity-band conduction[33] takes place. The holelike conduction observed at low temperatures is now attributed to this band and not the valence band. The Fermi energy is within the impurity band and the electron concentration in the conduction band will be zero at a pressure P_c for which E_g is equal to E_F. The values for the hole mobility at 4.2 °K of 76 and 78 $cm^2V^{-1}sec^{-1}$ (Table II) are typical of the magnitude obtained for this type of impurity-band conduction. This is not necessarily evidence for the model, however, since similar values would be expected for valence-band holes due to ionized impurity scattering at these impurity concentrations.

Other evidence for acceptor energies in the range 10–25 meV has been obtained for $Hg_{1-x}Cd_x$ Te, with x near 0.3, from Hall-effect and photoluminescence measurements.[13] Also, an unexplained line in the magnetoreflection data of Groves, Harman, and Pidgeon[5] would be consistent with a level situated approximately 20 meV above the valence-band edge.

The relatively low values for the electron mobility for samples 7B1 and 8B (Fig. 6) might also be expected since electrons at the Fermi surface can be scattered into the acceptor band states. We have not attempted an analysis of the pressure dependence of the mobility. We simply show in Fig. 6 the variation of $1/m^*_{eF}$ with pressure for the three samples, calculated using the values for E_0 and E_F given in Table II, where m^*_{eF} is the electron effective mass at the Fermi level. The electron effective mass is given by $m^*_e = \hbar^2 k (dE/dk)^{-1}$. Using the dispersion relation of Eq. (2) and k_F from Eq. (3), we obtain

$$\frac{m_0}{m^*_{eF}} = 1 + \frac{4P_K^2}{3\hbar^2}\, m_0 (E_g - 2E_F)^{-1} \quad . \tag{6}$$

It is apparent from Fig. 6 that the mobility variations cannot be accounted for by changes in the electron mass alone. The mobility for samples 7B1 and 8B varies more rapidly with pressure than $1/m^*_{eF}$, and the mobility for sample 7B shows a maximum which is not exhibited by $1/m^*_{eF}$.

The carrier concentrations in sample 7B at 77 °K are fitted quite well by the values calculated by using the Kane model (Fig. 5). However, the np products for samples 7B1 and 8B at 77 °K and zero pressure (Table I) are very high. Calculations using estimated values for E_0 yield values for np an order of magnitude lower than those obtained from the experimental values. We speculate that this is also due to the presence of an impurity band, the major part of the hole conduction in the samples occurring in the impurity band rather than the valence band. The presence of some valence-band conduction would account for the higher hole mobilities relative to the 4.2 °K values.

Measurements of the Hall coefficient at higher pressures, where the electron concentration is low, on samples 7B1 and 8B show a positive R falling with magnetic field initially (Figs. 3 and 7). This behavior can be accounted for by the presence of two sets of holes of different mobility, but to fit the magnetic field dependence the higher mobility set are required to have a mobility of order 10^4 $cm^2V^{-1}sec^{-1}$. One explanation[34] would be that the high mobility carriers are in the light-mass valence band, but since the positive Hall coefficient in sample 7B does not show the same behavior, we think that it is not correct.

The behavior of the longitudinal magnetoconductivity shown in Fig. 9 can also be explained using the model shown in Fig. 11. The conductivity is made up of two components which can be regarded as independent in this geometry: σ^e_{zz} due to electrons and σ^h_{zz} due to holes. At high pressures where the electron concentration is very small, $\sigma_{zz} \simeq \sigma^h_{zz}$